An Improved Reverse Flow Injection Analysis (rFIA) Technique for Determination of Nanomolar Concentrations of Ammonium in Natural Waters with Automatic Background Fluorescence Detection: Ammonification During a *Karenia brevis* Bloom in Tampa Bay

Robert T. Masserini Jr*[1], William Abbot[2], Hannah R. Hunt[3], Emily Friden[1], Cynthia A. Heil[4] Sarah M. Klass[4]

[1]*Department of Chemistry, Biochemistry, and Physics, The University of Tampa, 401 West Kennedy Boulevard, Tampa, Florida, 33606, USA Email: rmasserini@ut.edu, emily.friden@spartans.ut.edu.*

[2]*National Oceanic and Atmospheric Administration, Center for Operational Oceanographic Products and Services Pacific Operations Branch 7600 Sand Point Way NE Bldg. 8 Seattle, WA 98115, USA Email william.abbot@noaa.gov*

[3]*College of Marine Science, University of South Florida, 140 7th Ave. S., St. Petersburg, FL 33701, USA, Email: hannahhunt@usf.edu*

[4]*Mote Marine Laboratory, 1600 Ken Thompson Parkway Sarasota, Fl 34236, USA Email: cheil@mote.org, sklass@mote.org*

**corresponding author*

Keywords
ammonia, ammonium, fluorescence, fluorometric, nutrient, ocean, seawater, *Karenia brevis*, red tide, Tampa Bay, harmful algal bloom

Abstract

Ammonium is the most energetically favorable form of inorganic nitrogen that phytoplankton can take up, and its availability often limits phytoplankton biomass. Recently, the majority of methods for quantification of ammonium at nanomolar concentrations have used the reaction between ammonium and *o*-phthaldialdehyde (OPA). Two different approaches have been employed. One involves gas diffusion of ammonia across a membrane. The other entails a more direct approach and utilizes sulfite as a reducing agent to form a fluorescent product. A benefit of the separation technique is that natural fluorescence of the samples does not yield a false positive signal, however membrane failure and clogging are challenging analytical problems. The direct reaction between the analyte and OPA, although devoid of problems associated with membranes, requires a correction for background fluorescence. This work presents the development of a reverse flow injection analysis (rFIA) method with automatic background fluorescence correction and a low detection limit, along with its application to measure underway ammonium concentrations in Tampa Bay during a bloom of the toxic dinoflagellate *Karenia brevis* with concurrent fish kills in June of 2021. During field testing elevated concentrations of ammonium were found to coincide with the largest number of observed floating dead fish and lethal *K. brevis* concentrations. The method employs a sulfite-formaldehyde reagent mixed with the sample into which an OPA reagent is injected and heated

to activate fluorescence. Fluorescence of the sample is measured before the injection of OPA and at the peak of OPA injection, allowing for differentiation of the background fluorescence from the signal proportional to analyte. The detection limit and the limit of quantitation for this technique are 2.3 nM and 7.5 nM, respectively, and the coefficient of variation is 0.6 % for replicate deionized water blanks (N=10). Advantages of this method compared to techniques capable of both nanomolar detection of ammonium and improved accuracy via background fluorescence correction include a greater sample throughput, an increase in reported useful reagent lifetime, and the ability to quantify ammonium in coastal waters.

Introduction

Ammonium accounts for less than 1% of fixed nitrogen in surface waters, yet due to its reduced and energetically available nitrogen form, it can be responsible for up to 89% of photosynthetically assimilated nitrogen (Dortch, 1990; Pilson, 2013; Wheeler et al., 1989). When not replenished by autochthonous and allochthonous processes or upwelling, ammonium can subsequently be depleted in surface waters, resulting in oligotrophic regions with ammonium concentrations less than 1000 nM (Abbott, 2015; Johnson et al., 2008; Watson et al., 2005). Therefore, accurate quantification of the temporal and spatial variability of the ammonium that helps to drive net primary production is crucial for understanding both coastal processes and their impact on oceanic net primary production (Masserini et al., 2017).

Accurately measuring ammonium at nanomolar levels is especially important in oligotrophic southwest Florida coastal and estuarine waters. Blooms of the toxigenic dinoflagellate *Karenia brevis* occur almost annually in the eastern Gulf of Mexico, resulting in significant environmental destruction and negative effects on human health and local economies (Heil and Steidinger, 2009; Steidinger, 2009). These blooms which are especially prevalent in the region between Tarpon Springs and Ft. Myers, are generally considered to be limited by nitrogen (Heil et al., 2014; Vargo et al., 2008). Although 13 nutrient sources have been identified to support these *K. brevis* blooms (Heil et al., 2014; Vargo et al., 2008), ammonium and dissolved organic nitrogen derived from fish kills are the largest potential nitrogen source (Heil et al., 2014; Killberg-Thoreson et al., 2014; Walsh et al., 2009). Estimates of ammonium release from dead fish are based upon laboratory measurements (Killberg-Thoreson et al., 2014; Walsh et al., 2009), however few ammonium measurements exist in the vicinity of red tide related fish kills.

Reviews of the methods developed and optimized for ammonium in natural waters indicate that the vast majority of these techniques utilize either absorbance or fluorescence as the means of detection (Li et al., 2020; Ma et al., 2014; Molins-Legua et al., 2006; Šraj et al., 2014). Increasingly, the reaction of *o*-phthaldialdehyde (OPA) with ammonium has been explored for measurement of nanomolar ammonium concentrations using fluorescence detection. Table 1 summarizes representative fluorometric techniques for the determination of ammonium in natural waters using OPA. These analyses involve the reaction of ammonium with OPA in the presence of a reducing agent. Roth (1971) employed 2-mercaptoethanol as the reducing agent for the analysis of amino acids in seawater to produce a highly fluorescent compound. The introduction of a gas diffusion apparatus to separate ammonium from the sample increased the selectivity of the methodology for ammonium while decreasing impacts from amino-acid interferences and ionic strength related matrix effects (Lin et al., 2019; Šraj et al., 2014). Unfortunately, the transfer efficiency across the membrane is poor and can be variable (Zhu et al., 2013). Replacing 2-mercaptoethanol with sulfite resulted in higher selectivity for ammonium and eliminated the need for gas diffusion based separation while reintroducing the error associated with natural fluorescence of the sample contributing to analyte signal (Genfa and Dasgupta, 1989). A further improvement involved the addition of formaldehyde to the reaction to form a stable fluorescent α-hydroxymethanesulfonate complex resulting in a lower reagent blank and a greater selectivity for ammonium (Olson and Hoffmann, 1989). Complications with existing high sensitivity fluorescence-based techniques for ammonium measurements that can lead to inaccuracies are related to the natural fluorescence of dissolved organic matter, the reaction of OPA with primary amines and amino acids, and matrix effects that stem from

calibrations conducted with standards that do not match the ionic strength of the samples (Taylor et al., 2007).

Flow injection analysis (FIA) operates using a consistent reagent stream with short, reproducible injections of a sample. A set of guidelines for FIA were developed to help optimize and standardize FIA procedures (Růžička and Hansen, 1978). Reverse flow inejction introduces the sample to the flow-stream prior to the injection of the reagents (e.g. Masserini and Fanning, 2000). This approach decreases reagent use, increases reagent dispersion with the analyte, and allows for automated correction of background fluorescence from dissolved organic matter (DOM) in seawater. As depicted in Fig. 1, once a sample's background fluorescence achieves a plateau, the OPA reagent is injected to develop the fluorescent signal proportional to the ammonium present in the sample (steeper portion of the peak). The initial plateau height for a seawater sample results from fluorescence due to naturally occurring DOM, the difference between the refractive index of the sample and the deionized water (DIW) wash between samples, and any contaminant organic matter from the tubing used. Fluorescence is measured before and at the peak of the OPA injection, allowing the quantification and subtraction of background fluorescence from the signal proportional to the ammonium present in the sample. Following background correction, the reagent blank is also subtracted from all signals to yield the signal proportional to ammonium. As can be seen in Fig. 1 the background fluorescence can be significant and if not corrected for would lead to a positive. Abbot's (2015) thesis work provided the preliminary groundwork for a rFIA method; however these efforts did not evaluate potential interferences at optimized conditions, method sensitivity in freshwater, nor was it applied to samples. This study presents a fully characterized and field-tested automated rFIA fluorescence-based technique using the reaction between ammonium and OPA paired with a

sulfite-formaldehyde chemistry that improves the accuracy of nanomolar ammonium determinations. The field test of this method for the measurement of surface ammonium concentrations was conducted during the unusually destructive summer bloom of *K. brevis* in Tampa Bay in June of 2021.

Experimental

Reagents and Standards

All reagents were prepared in deionized water (DIW) that was polished to 18.2 MΩ-cm in an ARIES Filter Works High Purity Water System. All glassware and pipettes were rinsed with 1.2 M (10% V/V) hydrochloric acid followed by polished DIW three times to reduce atmospheric contamination. Reagents were stored in high-density polyethylene bottles. Standards were prepared daily and were held in custom polyvinylchloride (PVC) housings made to fit polyethylene baby bottle liners. The liners in the housing served as a compressible reservoir sealed with silicone o-rings which allowed for an air-tight system. The lids of the containers were manufactured to have a conical interior to assist with the removal of air from the housing. The lids were fit with valves (Omnifit 1101) and polytetrafluoroethylene (PTFE) adapters to limit atmospheric exposure.

The OPA reagent and the sodium sulfite-formaldehyde reagent were prepared using a 0.25 M tetraborate buffer with a pH of 9.5. The borate buffer was prepared by dissolving 30.92 g of boric acid (Fisher Scientific) in 2 L of polished DIW. The pH of the buffer solution was adjusted to 9.5 using 10 M sodium hydroxide (Fisher Scientific). The OPA was prepared by dissolving 0.7 g of OPA (Sigma-Aldrich) in 7 mL of methanol (Fisher Scientific) before adding the solution to 1 L of the buffer solution. The sodium sulfite-formaldehyde reagent was prepared by

dissolving 1.27 g sodium sulfite in 1 L of tetraborate buffer followed by adding 350 µL of formaldehyde (Fisher Scientific).

Standard solutions were prepared using gravimetrically calibrated glassware and pipettes. Ammonium chloride (Sigma-Aldrich) that was dried at 105°C for two hours was used for the preparation of 25 mM primary standards of ammonium. The secondary standard was made by diluting 10 mL of primary standard in a 1000 mL volumetric flask with polished DIW. Working standards were prepared daily from the secondary standard stock solutions using a 250 mL volumetric flask.

Interference Solutes

Increased selectivity of OPA for ammonium over amines and amino acids when using a sulfite-formaldehyde reagent has been reported previously (Abi Kaed Bey et al., 2011; Amornthammarong and Zhang, 2008; Kérouel and Aminot, 1997) and the species most likely to interfere were selected based upon those studies. All reagents used for the interference study came from Sigma Aldrich. Amino acid and primary amine standard solutions of ethanolamine, L-serine, L-tyrosine, L-leucine, L-phenylalanine, L-tryptophan, L-alanine, and beta-alanine (all $2.5x10^{-4}$ M) were made in polished DIW. 1000 nM solutions of each interfering specie were then prepared in polished DIW, and the interferences of amino acids and primary amines on the method response were determined by running triplicates.

Salinity Interferences

Seven solutions of varying salinities (S = 0.0, 3.0, 7.0, 13.0, 22.0, 30.0, and 39.0) were prepared by mixing different proportions of low nutrient seawater (LNSW) and polished DIW. The aged LNSW had a background ammonium concentration of 3.3 nM as determined via standard additions, and the solvent background ammonium contribution was subtracted from all

calibrants. Calibration curves were performed using the varying salinities as the solvents. The slope of each calibration curve was determined to analyze the effect of increasing salinity on the response of the methodology.

rFIA Manifold Description

The analytical manifold for ammonium determination is diagramed in Fig. 2. A peristaltic pump was used to draw the wash, sample, standards, and reagents from their compressible reservoirs and flowrates for the OPA reagent, sample, sulfite reagent, and waste draw were 0.5, 0.9, 0.9 and 2.1 mL min^{-1}, respectively. The PVC pump tubes were connected to the 0.8 mm inner diameter PTFE tubing with ¼ inch-28 threaded flange fittings polyether ether ketone tees (VICI Valco instruments CTMPK). The tubing lengths are a replica of the rFIA manifold used for nitrite analysis described in Masserini et al. (2017)

The valves were controlled by valve-coupled stepper motors with actuators. A local operating network module connected to the valve actuator enabled autonomous control of the 200s valve cycle. The first 60 seconds of the cycle was the wash phase. DIW was directed through the sample stream selection valve (VICI Cheminert), and the reagent stream was directed to waste. At 60 seconds, the analyte stream was directed to a tee where the sulfite-formaldehyde reagent was introduced. At 185s, 0.15 mL of the OPA reagent was injected, and the sample was directed towards the heater. At 200s, the valve returns to the wash position and completes the valve cycle which yields a sample throughput of 18 samples hr^{-1}. During the rFIA processing of a sample a sulfite-formaldehyde reagent is mixed with the sample stream and then injected with the OPA reagent before being heated.

Temperature was maintained (± 0.1 °C) with a proportional-integral-derivative controller (Watlow Anafaz 4CLS). 400 cm of PTFE tubing was coiled around an aluminum rod with a

heating element in the center and the analyte stream was warmed by contact. Fluorescence of the analyte stream was monitored with a Hitachi L-7480 fluorimeter outfitted with a 40 µL quartz flow cell and excitation and emission wavelengths of 365 nm and 425 nm, respectively. Photomultiplier tube sensitivity and signal averaging were both set to 2.

Results and Discussion

Optimization

The effect of temperature on the response of the chemistry was determined by running a calibration curve (DIW, LNSW, 300 nM, 600 nM, and 1000 nM in triplicate) at six discreet temperatures (45℃, 50℃, 55℃, 60℃, 65℃, and 70℃), and a salinity of 39. At 70℃ microbubbles were observed due to outgassing of dissolved gases, therefore a temperature of 65℃ was selected because it gave sufficient sensitivity, and no microbubbles were observed. Fig. 3 presents the slope of the calibration curve for each temperature. The data presented in Fig. 3 suggests that there is a strong correlation between temperature and sensitivity (slope). The effect of salinity on the slope of the calibration curve was also determined by running a calibration curve (DIW, LNSW, 300 nM, 600 nM, and 1000 nM in triplicate) using seven batches of diluted LNSW as the solvent (S=0.0, 3.0, 7.0, 13.0, 22.0, 30.0, and 39.0) at 65℃. The results can be seen in Fig. 4 and indicate there is minimal influence of salinity on sensitivity.

Standard Curve

Working standards were prepared in LNSW as described above. The standardization used for Fig. 5 was a sequence of triplicate injections consisting of DIW, LNSW, 200 nM, 400 nM, 600 nm, and 800 nm calibrants. The calibration curve is plotted in Fig. 6.

Figures of Merit

The figures of merit, including the limit of detection (LOD), limit of quantitation (LOQ), limit of linearity (LOL), and coefficient of variation (CV), are summarized in Table 2. The LOD was calculated by multiplying the standard deviation of the DIW blank peaks (N =10) by a factor of three. The LOD for this methodology is 2.3 nM (Table 2). The limit of quantitation was calculated as ten times the standard deviation of the DIW blanks.

Interferences

The interferences of amino acids and primary amines on the response of the method were determined by running triplicates of 1000 nM solutions of each the interfering species listed in Table 3. The concentration of amino acids and primary amines rarely exceeds 50 nM in the environment (Suttle et al., 1991), which was 20 times less than the tested interfering species concentrations. Therefore, the signal obtained for each 1000 nM interfering specie solution was divided by 20 to determine the largest likely potential interference that might be seen in natural water samples. The contribution of these amino acids and primary amines to the measured fluorescence is less than the LOQ (7.5 nM) except for L-phenylalanine and L-tryptophan which were estimated to be 7.6 and 8.7 nM, respectively. Therefore, it is unlikely that these potential interferants would contribute significantly to the quantitation of ammonium. The observed selectivity of OPA for ammonium over amines and amino acids when using a sulfite-formaldehyde reagent is in agreement with previous studies (Abi Kaed Bey et al., 2011; Adornato et al., 2007; Aminot et al., 2001; Dzaugis et al., 2018; Genfa and Dasgupta, 1989) .

Reagent Stability

Reagent stability was evaluated by conducting calibrations at 0, 16, 48, and 55 days from the date of reagent preparation. Fig. 7 presents the slopes of the calibration curves. The slope of the

calibration curves increased with time except for the final data point. This decrease may be indicative of the beginnings of reagent degradation. Given the 2.7 times enhancement in sensitivity over 16 days we suggest preparing reagents in advance if possible and monitoring calibrations after every three hours of operation. The reagents described herein provided a working life greater than 50 days while techniques which employ similar reagents have reported reagent stability on the order of weeks (Abi Kaed Bey et al., 2011; Amornthammarong and Zhang, 2008). In comparison, OPA reagents made with 2-mercaptoethanol can take 48 hours for the reagent fluorescence to decrease to the point where the solution can even be used, and then only work for another 48 hours thereafter while being notoriously unstable (Dorresteijn et al., 1996). These results indicate that the OPA and sulfite reagents described herein have a working life that is over three times greater than those previously reported and at least 10 times greater than 2-mercaptoethanol based reagents.

Field Study

A cruise was conducted in eastern Tampa Bay on June 22, 2021 to demonstrate the capabilities of the methodology and investigate the influence of localized floating aggregations of dead fish on surface ammonium concentrations. A bloom of *K. brevis* was present in Tampa Bay from May through October of 2021, with associated fish kills (as dead fish of multiple species floating at the water surface) observed throughout Tampa Bay during June and July of 2021, including the day of the cruise. As depicted in Fig. 8a, the transect began in Hillsborough Bay (HB) and traveled through Middle Tampa Bay (MTB) and into Lower Tampa Bay (LTB) on the 12 m *R/V BIOS II*. Sample collection started at approximately 9AM local time during slack tide and continued for six hours with an incoming tide up until noon. The rFIA method was integrated into the C-SWANN (Masserini et al. 2017) so that sample position data could be acquired along

with ammonium concentrations. Behind the vessel an aluminum planar tow body was attached to a high-density polyethylene tube which was hauled at approximately 7.4 kilometers per hour. Water from the upper 1 m of the bay was pumped up to the vessel at approximately 10 L/minute. On the inlet side, the water was strained through a stainless steel 50 mesh filter while a 25-micron microporous polyethylene filter was placed on the outlet side pump which provided the source water for ammonium determinations. One sample was injected every 200 s or about every 410 m. While the vessel was underway, estimates of the abundance of dead fish were made concurrently with sampling for *K. brevis*. Visible dead marine life was counted in a 20 m wide swath along the path of the vessel (10 m on either side). These counts were continuously taken throughout the transect and divided into 15-minute sections to align with the *K. brevis* sampling. Whole water samples for determination of *K. brevis* concentrations were collected at the outlet side of the pumping system, prior to the 25 micron filter, in 15 ml clean glass scintillation vials containing 0.5 ml of Lugol's preservative and stored in the dark (Tomas, 1997). Cell concentrations were determined using a Sedgewick-Rafter counting chamber and a Zeiss Primo-Start Compound Microscope. Phytoplankton were identified to the species level where possible according to Tomas (1997) with *Karenia* species identification based on cell morphology and nuclear placement.

Ammonium concentrations generally increased as the vessel moved south in the bay (see Fig. 8b). The average ammonium concentration was 34 nM and the maximum ammonium concentration was present in MTB at 67 nM. Although the 12 m research vessel did not have a scientific seawater system, salinity and temperature data were available from a sensor suite maintained in the region at 27° 39.7 N and 82° 36.0 W ("Tampa Bay Land/Ocean Biogeochemical Observatory," 2022) depicted as a green triangle in Fig. 8a. The observatory

reported an average practical salinity of 33.81 with a range of 1.09 (33.07 to 34.16). Given the method's sensitivity stability in this range of salinities, impact of salinity on ammonium quantification is unlikely. Similarly, the average water temperature during the sampling period was 29.47 ℃ with a range of less than half a degree (29.27 to 29.70 ℃). The fish kill count was highest in MTB with 28 dead fish observed over 2.4 kilometers out of 50 total dead fish encountered over the entire cruise (see Fig. 8c). Deceased species observed included *Mugil gyrans, Mugil cephalus, Bagre marinus, Mycteroperca microlepis, Lutjanus griseus, Paralichthys albigutta, Paralichthys dentatus, Arius Felis, Lagodon rhomboides, Cynoscion nebulosus,* and *Anguilla rostrata*. Maximum *K. brevis* concentrations were present on the border between HB and MTB as seen in Fig. 8d. The average and maximum *K. brevis* cell concentrations were 5.8 x 10^5 cells L^{-1} and 3.2 x 10^6 cells L^{-1}, respectively. There were only 4 samples containing *K. brevis* concentrations less than 2.5 x 10^5 cells L^{-1} during the survey, well within the lower range reported for fish mortality (Pierce and Henry, 2008).

Unfortunately, reagent reservoirs were being refilled where the highest *K. brevis* concentrations were observed, and therefore limited ammonium data is available in this region. Compared to ambient concentrations outside the enrichment region, an ammonium supplementation of 33 nM was quantified in a volume of approximately 1.6 x 10^5 m^3. It is notable that this region is also where the greatest mortality was observed. This would require a net augmentation of approximately 9.5 x 10^{-2} kg of ammonium to be released into the water column above that potentially removed from diffusion, advection, and reaction.

The pervasiveness of *K. brevis* throughout the survey area is unusual for several reasons. Generally, *K. brevis* is not found at S<24 (Maier Brown et al., 2006) and blooms are usually restricted from the middle to upper regions of Tampa Bay by lower salinities. An extended

drought period led to high summer salinities in Tampa Bay and allowed for expansion of the *K. brevis* bloom into HB coincident with reduced freshwater riverine inputs (Beck et al., 2022). Blooms of *K. brevis* are also unusual in the summer months, generally blooms initiate in early fall and terminate by the following April (Heil et al., 2021). A late initiating bloom in December 2020 overwintered in coastal waters and then spread to and intensified through the summer of 2021 within Tampa Bay, which has only been recorded before in 1963, 1971, 2005, 2018 and 2021 (K. Steidinger, pers. comm.).

Nutrients derived from the decay of dead fish have been identified as the largest nutrient source of both nitrogen and phosphorus for blooms of the 13 different sources identified (Heil et al., 2014; Vargo et al., 2008) and fish decay was likely rapid given the warm summer water temperatures in the study area. Although the association between elevated ammonium concentrations, *K. brevis* and dead fish is correlative, the severely nitrogen limited nature of Tampa Bay (Greening et al., 2014; Sherwood et al., 2016), the low ammonium concentrations throughout upper Tampa Bay during the survey period, the elevated concentrations of *K. brevis* observed during the current survey and though out Tampa Bay during June and July of 2021, the floating dead fish observed in the vicinity of the transect (Fig. 8c), as well as the >1,600 tons of dead fish removed from local beaches in June and July of 2021 (Beck et al., 2022) all support the decay of dead fish as the cause of elevated ammonium levels observed during the survey.

Conclusions

The methodology described above enhances the accuracy of nanomolar ammonium determinations by automatically correcting for the background fluorescence of each sample. Automatic background correction removes the positive bias associated with other direct fluorescent methods, and the removal of the gas diffusion membrane reduces sources of error

associated with membrane instability. A greater sample throughput and an increase in reagent lifetime are additional advantages. Furthermore, this improved methodology successfully quantified nanomolar ammonium enrichment in the surface waters of Tampa Bay that correlated with the maximum localized fish kills surveyed during a bloom of the toxic dinoflagellate *K. brevis*. It is therefore likely that this subtle enrichment can only be detected with high-sensitivity high-resolution monitoring.

Acknowledgements

This research was supported by the University of Tampa's Summer Undergraduate Research Fellowship (Grant # 3098) and the Research Innovation and Scholarly Excellence Award (Grant # 1920), NOAA Ecohab Program (Grant#NA19NOS4780183) and the Florida Red Tide Mitigation and New Technology Development Initiative. Dr. Kelly Diester and the reviewers are thanked for their insightful feedback on this manuscript. We thank the University of Tampa's College of Natural and Health Sciences for ship time on the *R/V BIOS II*. Marlena Penn is thanked for her efforts during optimization and suggestions. We also thank John Ambrosio, Captain Harry Conners, Alynne Holmstrom, Bailey Lake, William Love, and Ethan Vallebuona for their assistance during the field study. This is ECOHAB Publication #1025.

Abbott, W., 2015. The Development of a Fluorescence-based Reverse Flow Injection Analysis (rFIA) Method for Quantifying Ammonium at Nanomolar Concentrations in Oligotrophic Seawater.

Abi Kaed Bey, S.K., Connelly, D.P., Legiret, F.E., Harris, A.J.K., Mowlem, M.C., 2011. A high-resolution analyser for the measurement of ammonium in oligotrophic seawater. Ocean Dyn. 61, 1555–1565. https://doi.org/10.1007/s10236-011-0469-5

Adornato, L.R., Kaltenbacher, E.A., Greenhow, D.R., Byrne, R.H., 2007. High-resolution in situ analysis of nitrate and phosphate in the oligotrophic ocean. Environ. Sci. Technol. 41, 4045–4052. https://doi.org/10.1021/es0700855

Aminot, A., Kérouel, R., Birot, D., 2001. A flow injection-fluorometric method for the determination of ammonium in fresh and saline waters with a view to in situ analyses. Water Res. 35, 1777–1785. https://doi.org/10.1016/S0043-1354(00)00429-2

Amornthammarong, N., Zhang, J.Z., 2008. Shipboard fluorometric flow analyzer for high-resolution underway measurement of ammonium in seawater. Anal. Chem. 80, 1019–1026. https://doi.org/10.1021/ac701942f

Beck, M.W., Altieri, A., Angelini, C., Burke, M.C., Chen, J., Chin, D.W., Gardiner, J., Hu, C., Hubbard, K.A., Liu, Y., Lopez, C., Medina, M., Morrison, E., Phlips, E.J., Raulerson, G.E., Scolaro, S., Sherwood, E.T., Tomasko, D., Weisberg, R.H., Whalen, J., 2022. Initial estuarine response to inorganic nutrient inputs from a legacy mining facility adjacent to Tampa Bay, Florida. Mar. Pollut. Bull. 178, 113598. https://doi.org/10.1016/j.marpolbul.2022.113598

Dorresteijn, R.C., Berwald, L.G., Zomer, G., De Gooijer, C.D., Wieten, G., Beuvery, E.C., 1996. Determination of amino acids using o-phthalaldehyde-2-mercaptoethanol derivatization: Effect of reaction conditions. J. Chromatogr. A 724, 159–167. https://doi.org/10.1016/0021-9673(95)00927-2

Dortch, Q., 1990. The interaction between ammonium and nitrate uptake in phytoplankton. Mar. Ecol. Prog. Ser. 61, 183–201. https://doi.org/10.3354/meps061183

Dzaugis, M., Spivack, A.J., D'Hondt, S., 2018. Radiolytic H $_2$ Production in Martian Environments. Astrobiology 18, 1137–1146. https://doi.org/10.1089/ast.2017.1654

Genfa, Z., Dasgupta, P.K., 1989. Fluorometric Measurement of Aqueous Ammonium Ion in a Flow Injection System. Anal. Chem. 61, 408–412. https://doi.org/10.1021/ac00180a006

Giakisikli, G., Anthemidis, A.N., 2018. Automatic pressure-assisted dual-headspace gas-liquid microextraction. Lab-in-syringe platform for membraneless gas separation of ammonia coupled with fluorimetric sequential injection analysis. Anal. Chim. Acta 1033, 73–80. https://doi.org/10.1016/j.aca.2018.06.034

Giakisikli, G., Trikas, E., Petala, M., Karapantsios, T., Zachariadis, G., Anthemidis, A., 2017. An integrated sequential injection analysis system for ammonium determination in recycled hygiene and potable water samples for future use in manned space missions. Microchem. J. 133, 490–495. https://doi.org/10.1016/j.microc.2017.04.008

Greening, H., Janicki, A., Sherwood, E.T., Pribble, R., Johansson, J.O.R., 2014. Ecosystem responses to long-term nutrient management in an urban estuary: Tampa Bay, Florida, USA. Estuar. Coast. Shelf Sci. 151, A1–A16. https://doi.org/10.1016/j.ecss.2014.10.003

Heil, C.A., Amin, S.A. , Glibert, P. M Hubbard, K.A. Li, M., Martinez-Martinez, J. Weisberg, R., Liu, Y., Sun, Y., 2021. Termination patterns of Karenia brevis blooms in the eastern Gulf of Mexico, in: Proceedings of the 19th International Conference on Harmful Algae. La Paz, Mexio.

Heil, C.A., Dixon, L.K., Hall, E., Garrett, M., Lenes, J.M., O'Neil, J.M., Walsh, B.M., Bronk, D.A., Killberg-Thoreson, L., Hitchcock, G.L., Meyer, K.A., Mulholland, M.R., Procise, L., Kirkpatrick, G.J., Walsh, J.J., Weisberg, R.W., 2014. Blooms of Karenia brevis (Davis) G. Hansen & Ø. Moestrup on the West Florida Shelf: Nutrient sources and potential management strategies based on a multi-year regional study. Harmful Algae 38, 127–140. https://doi.org/10.1016/j.hal.2014.07.016

Heil, C.A., Steidinger, K.A., 2009. Monitoring, management, and mitigation of Karenia blooms in the eastern Gulf of Mexico. Harmful Algae 8, 611–617. https://doi.org/10.1016/j.hal.2008.11.006

Holmes, R.M., Aminot, A., Kérouel, R., Hooker, B.A., Peterson, B.J., 1999. A simple and precise method for measuring ammonium in marine and freshwater ecosystems. Can. J. Fish. Aquat. Sci. 56, 1801–1808. https://doi.org/10.1139/f99-128

Horstkotte, B., Duarte, C.M., Cerd, V., 2011. A miniature and field-applicable multipumping flow analyzer for ammonium monitoring in seawater with fluorescence detection. Talanta 85, 380–385. https://doi.org/10.1016/j.talanta.2011.03.078

Hu, H., Liang, Y., Li, S., Guo, Q., Wu, C., 2014. A modified o -phthalaldehyde fluorometric analytical method for ultratrace ammonium in natural waters using edta-naoh as buffer. J. Anal. Methods Chem. 2014. https://doi.org/10.1155/2014/728068

Johnson, M.T., Liss, P.S., Bell, T.G., Lesworth, T.J., Baker, A.R., Hind, A.J., Jickells, T.D., Biswas, K.F., Woodward, E.M.S., Gibb, S.W., 2008. Field observations of the ocean-atmosphere exchange of ammonia: Fundamental importance of temperature as revealed by a comparison of high and low latitudes. Global Biogeochem. Cycles 22. https://doi.org/10.1029/2007GB003039

Jones, R.D., 1991. An improved fluorescence method for the determination of nanomolar concentrations of ammonium in natural waters. Limnol. Oceanogr. 36, 814–819. https://doi.org/10.4319/lo.1991.36.4.0814

Kérouel, R., Aminot, A., 1997. Fluorometric determination of ammonia in sea and estuarine waters by direct segmented flow analysis. Mar. Chem. 57, 265–275. https://doi.org/10.1016/S0304-4203(97)00040-6

Killberg-Thoreson, L., Sipler, R.E., Heil, C.A., Garrett, M.J., Roberts, Q.N., Bronk, D.A., 2014. Nutrients released from decaying fish support microbial growth in the eastern Gulf of Mexico. Harmful Algae 38, 40–49. https://doi.org/10.1016/j.hal.2014.04.006

Li, D., Xu, X., Li, Z., Wang, T., Wang, C., 2020. Detection methods of ammonia nitrogen in water: A review. TrAC - Trends Anal. Chem. https://doi.org/10.1016/j.trac.2020.115890

Lin, K., Zhu, Y., Zhang, Y., Lin, H., 2019. Determination of ammonia nitrogen in natural waters: Recent advances and applications. Trends Environ. Anal. Chem. 24, e00073. https://doi.org/10.1016/J.TEAC.2019.E00073

Ma, J., Adornato, L., Byrne, R.H., Yuan, D., 2014. Determination of nanomolar levels of nutrients in seawater. TrAC - Trends Anal. Chem. https://doi.org/10.1016/j.trac.2014.04.013

Maier Brown, A.F., Dortch, Q., Dolah, F.M.V., Leighfield, T.A., Morrison, W., Thessen, A.E., Steidinger, K., Richardson, B., Moncreiff, C.A., Pennock, J.R., 2006. Effect of salinity on the distribution, growth, and toxicity of Karenia spp. Harmful Algae 5, 199–212. https://doi.org/10.1016/j.hal.2005.07.004

Masserini, R.T., Fanning, K.A., 2000. A sensor package for the simultaneous determination of nanomolar concentrations of nitrite, nitrate, and ammonia in seawater by fluorescence

detection. Mar. Chem. 68, 323–333. https://doi.org/10.1016/S0304-4203(99)00088-2
Masserini, R.T., Fanning, K.A., Hendrix, S.A., Kleiman, B.M., 2017. A coastal surface seawater analyzer for nitrogenous nutrient mapping. Cont. Shelf Res. 150, 48–56. https://doi.org/10.1016/j.csr.2017.09.010
Molins-Legua, C., Meseguer-Lloret, S., Moliner-Martinez, Y., Campíns-Falcó, P., 2006. A guide for selecting the most appropriate method for ammonium determination in water analysis. TrAC - Trends Anal. Chem. 25, 282–290. https://doi.org/10.1016/j.trac.2005.12.002
Olson, T.M., Hoffmann, M.R., 1989. Hydroxyalkylsulfonate formation: Its role as a S(IV) reservoir in atmospheric water droplets. Atmos. Environ. 23, 985–997. https://doi.org/10.1016/0004-6981(89)90302-8
Pierce, R.H., Henry, M.S., 2008. Harmful algal toxins of the Florida red tide (Karenia brevis): Natural chemical stressors in South Florida coastal ecosystems. Ecotoxicology 17, 623–631. https://doi.org/10.1007/s10646-008-0241-x
Pilson, M.E.Q., 2013. An introduction to the chemistry of the sea. Cambridge University Press.
Roth, M., 1971. Fluorescence Reaction for Amino Acids. Anal. Chem. 43, 880–882. https://doi.org/10.1021/ac60302a020
Růžička, J., Hansen, E.H., 1978. Flow injection analysis. Anal. Chim. Acta 99, 37–76. https://doi.org/10.1016/S0003-2670(01)84498-6
Schlitzer, R., 2021. Ocean Data View, http://odv.awi-bremerhaven.de, [WWW Document]. URL http://odv.awi.de
Sherwood, E.T., Greening, H.S., Janicki, A.J., Karlen, D.J., 2016. Tampa Bay estuary: Monitoring long-term recovery through regional partnerships. Reg. Stud. Mar. Sci. 4, 1–11. https://doi.org/10.1016/j.rsma.2015.05.005
Šraj, L.O., Almeida, M.I.G.S.S., Swearer, S.E., Kolev, S.D., Mckelvie, I.D., 2014. Analytical challenges and advantages of using flow-based methodologies for ammonia determination in estuarine and marine waters. TrAC Trends Anal. Chem. 59, 83–92. https://doi.org/10.1016/j.trac.2014.03.012
Steidinger, K.A., 2009. Historical perspective on Karenia brevis red tide research in the Gulf of Mexico. Harmful Algae 8, 549–561. https://doi.org/10.1016/j.hal.2008.11.009
Suttle, C., Chan, A., Fuhrman, J., 1991. Dissolved free amino acids in the Sargasso Sea: uptake and respiration rates, turnover times, and concentrations. Mar. Ecol. Prog. Ser. 70, 189–199. https://doi.org/10.3354/meps070189
Tampa Bay Land/Ocean Biogeochemical Observatory [WWW Document], 2022. https://doi.org/10.5066/P9BAFC7L.
Taylor, B.W., Keep, C.F., Hall, R.O., Koch, B.J., Tronstad, L.M., Flecker, A.S., Ulseth, A.J., 2007. Improving the fluorometric ammonium method: Matrix effects, background fluorescence, and standard additions. J. North Am. Benthol. Soc. 26, 167–177. https://doi.org/10.1899/0887-3593(2007)26[167:ITFAMM]2.0.CO;2
Tomas, C.., 1997. Identifying marine phytoplankton. Elsevier.
Vargo, G.A., Heil, C.A., Fanning, K.A., Dixon, L.K., Neely, M.B., Lester, K., Ault, D., Murasko, S., Havens, J., Walsh, J., Bell, S., 2008. Nutrient availability in support of Karenia brevis blooms on the central West Florida Shelf: What keeps Karenia blooming? Cont. Shelf Res. 28, 73–98. https://doi.org/10.1016/j.csr.2007.04.008
Walsh, J.J., Weisberg, R.H., Lenes, J.M., Chen, F.R., Dieterle, D.A., Zheng, L., Carder, K.L., Vargo, G.A., Havens, J.A., Peebles, E., Hollander, D.J., He, R., Heil, C.A., Mahmoudi, B., Landsberg, J.H., 2009. Isotopic evidence for dead fish maintenance of Florida red tides,

with implications for coastal fisheries over both source regions of the West Florida shelf and within downstream waters of the South Atlantic Bight. Prog. Oceanogr. 80, 51–73. https://doi.org/10.1016/j.pocean.2008.12.005

Wang, C., Li, Z., Pan, Z., Li, D., 2018. Development and characterization of a highly sensitive fluorometric transducer for ultra low aqueous ammonia nitrogen measurements in aquaculture. Comput. Electron. Agric. 150, 364–373. https://doi.org/10.1016/j.compag.2018.05.011

Watson, R.J., Butler, E.C. V, Clementson, L.A., Berry, K.M., 2005. Flow-injection analysis with fluorescence detection for the determination of trace levels of ammonium in seawater. J. Environ. Monit. 7, 37–42. https://doi.org/10.1039/b405924g

Wheeler, P.A., Kirchman, D.L., Landry, M.R., Kokkinakis, S.A., 1989. Diel periodicity in ammonium uptake and regeneration in the oceanic subarctic Pacific: Implications for interactions in microbial food webs. Limnol. Oceanogr. 34, 1025–1033. https://doi.org/10.4319/lo.1989.34.6.1025

Xue, S., Uchiyama, K., Li, H. fang, 2012. Determination of ammonium on an integrated microchip with LED-induced fluorescence detection. J. Environ. Sci. 24, 564–570. https://doi.org/10.1016/S1001-0742(11)60802-4

Zhu, Y., Chen, J., Shi, X., Yuan, D., Feng, S., Zhou, T., Huang, Y., 2018. Development and application of a portable fluorescence detector for shipboard analysis of ammonium in estuarine and coastal waters. Anal. Methods 10, 1781–1787. https://doi.org/10.1039/c8ay00438b

Zhu, Y., Yuan, D., Huang, Y., Ma, J., Feng, S., 2013. A sensitive flow-batch system for on board determination of ultra-trace ammonium in seawater: Method development and shipboard application. Anal. Chim. Acta 794, 47–54. https://doi.org/10.1016/j.aca.2013.08.009

Zhu, Y., Yuan, D., Lin, H., Zhou, T., 2016. Determination of ammonium in seawater by purge-and-trap and flow injection with fluorescence detection. Anal. Lett. 49, 665–675. https://doi.org/10.1080/00032719.2015.1041027

Table 1. An overview of fluorometric techniques for the determination of ammonium in natural waters using OPA (1971-2019).

Chemistry	Technique	$\lambda_{ex}/\lambda_{em}$ (nm)	Figures of Merit	Application	Reference
OPA-2-mercaptomethanol, tetraborate buffer pH=9.5	Manual	340/445	LOD: nanomole throughput: 25 samples h^{-1}	analysis of amino acids	(Roth, 1971)
OPA-2-mercaptoethanol, borate buffer pH = 9.5, 35 ℃	GD-FIA	335/470	LOD: < 1.5 nM NH_4^+ linear >2000 nM throughput: 30 samples h^{-1}	freshwater, seawater	(Jones, 1991)
OPA-2-mercaptoethanol, borate buffer pH = 9.5, 35 ℃	GD-FIA	335/470	LOD: ~ 1.0 nM NH_4^+ throughput: 18 samples h^{-1}	shipboard, seawater	(Masserini and Fanning, 2000)
OPA-sulfite, phosphate buffer, pH = 11.0, 85 ℃	FIA	360/420	LOD: 20 nM NH_4^+ linear: 0.25-20 μM NH_4^+ throughput: 25 samples h^{-1}	rainwater	(Genfa and Dasgupta, 1989)
OPA-sulfite, tetraborate buffer, pH = 9-9.5, 35 ℃	SFA	365/425	LOD: 1.5 nM NH_4^+ linear: <12 μM NH_4^+ throughput: 20 samples h^{-1}	estuarine, seawater	(Kérouel and Aminot, 1997)
OPA-sulfite, tetraborate buffer	Manual	350/420	LOD: 31 nM NH_4^+ linear: <6.2 μM NH_4^+ throughput: 3 hr $sample^{-1}$	field and lab protocol	(Holmes et al., 1999)
OPA-sulfite Tetraborate buffer, 30 ℃	FIA/Stop-Flow	370/418	LOD: 30 nM NH_4^+ linear: <50 μM NH_4^+ throughput: 9 samples h^{-1}	coastal, estuarine, freshwater	(Aminot et al., 2001)
OPA-sulfite, tetraborate buffer, pH = 9.4, 65 ℃	FIA	370/427	LOD: <5 nM NH_4^+ linear: 1 μM NH_4^+ throughput: 12 samples h^{-1}	field protocol, seawater	(Abi Kaed Bey et al., 2011)
OPA-sulfite phosphate buffer pH = 9.3, 70 ℃	GD-FIA	310/390	LOD: 7 nM NH_4^+ linear: < 4 μM NH_4^+ throughput: 30 samples h^{-1}	seawater	(Watson et al., 2005)
OPA-sulfite-formaldehyde, no buffer, pH = 11, 65 ℃	FIA/cFIA	363/423	LOD: 1.1 nM NH_4^+ linear: <600 nM NH_4^+ throughput: 8 samples h^{-1}	shipboard, seawater	(Amornthammarong and Zhang, 2008)
OPA-sulfite-formaldehyde, phosphate buffer pH = 11, 60 ℃	LIS	365/425	LOD: 0.05 µg L^{-1} NH_4^+ linear: <10µg L^{-1} NH_4^+ throughput 8 sample h^{-1}	river, lake, tap, ditch, seawater water	(Giakisikli and Anthemidis, 2018)
OPA-sulfite Phosphate buffer pH=11, 70ºC	SIA	365/425	LOD: 0.018 mg L^{-1} $NH4^+$ linear: 0.06-4.00 mgL^{-1} NH_4^+ throughput 20 sample h^{-1}	recycled water	(Giakisikli et al., 2017)
OPA, sodium tetraborate, sodium sulfite, no buffer, 82ºC	FIA	365/425	LOD: 13 nM NH_4^+ linear: <1 μM NH_4^+ throughput 32 sample h^{-1}	seawater	(Horstkotte et al., 2011)

OPA-sulfite-formaldehyde, EDTA-NaOH buffer pH= 10.80-11.70,	FIA	361/423	LOD: 0.0099 μM NH_4^+ Linear: 0.032-0.500, 0.250-3.00, and 1.00- 20.0 μM NH_4^+	natural waters	(Hu et al., 2014)
OPA-sulfite, borate buffer, 25ºC	FIA	365/430	LOD: 0.16 μg·L^{-1} NH_4^+ linear: <419.31 μg·L^{-1}	natural waters	(Wang et al., 2018)
OPA-sulfite, phosphate buffer pH= 10.5	FIA	365/425	LOD: 3.6 × 10−4 μg mL^{-1} NH_4^+ linear: 0.018 -1.8 μg mL^{-1} NH_4^+	rain, river water	(Xue et al., 2012)
OPA-sulfite, borate buffer	FIA	368/429	LOD: 2.1 nM NH_4^+ linear: <300 nM NH_4^+ throughput 36 sample h^{-1}	estuarine and coastal water	(Zhu et al., 2018)
Phosphate buffer, 75ºC	Flow batch SPE	362/423	LOD: 0.7 nM NH_4^+ linear: 1.67–300 nM NH_4^+ throughput 5 sample h^{-1}	seawater	(Zhu et al., 2013)
OPA-sulfite, carbonate buffer pH 13.2, 80ºC	FIA and PT	not published	LOD: 7.4 nM NH_4^+ linear: 10-400 nM NH_4^+	seawater	(Zhu et al., 2016)
OPA-sulfite-formaldehyde, borate buffer pH = 9.5, 65 ℃	rFIA	365/425	LOD: 2.3 nM NH_4^+ linear: <7000 nM NH_4^+ throughput 18 samples h^{-1}	natural waters	This method

Lab-in-syringe (LIS)
Sequential injection analysis (SIA)
Solid Phase Extraction (SPE)
Purge and Trap (PT)

Table 2. Figures of Merit.

Figures of Merit	
LOD (nM)	2.3
LOQ (nM)	7.5
LOL (nM)	7000
CV (%)	0.6

Table 3. Potential primary amine and amino acid interferences.

Primary Amine, Amino Acid	Ammonium Equivalence (nM) of 1 μM Interfering Species	Ammonium Equivalence (nM) of 50 nM Interfering Species
Ethanolamine	32.4±1.8	1.62
L-Serine	58.3±0.7	2.92
L-Tyrosine	49.8±0.3	2.49
L-Leucine	49.1±0.7	3.46
L-Phenylalanine	152.3±6.1	7.62
L-Tryptophan	175.0±1.4	8.75
L-Alanine	20.6±2.3	1.03
Beta-Alanine	95.5±2.3	4.78

Figure Legends

Fig. 1. rFIA background fluorescence. The relative response of a reagent blank prepared in deionized water (DIW, blue) and a solvent blank consisting of low nutrient seawater (LNSW, orange) shows the background fluorescence from dissolved organic matter present in seawater once the sample enters the fluorometer from 20-100 s before OPA is injected and mixed from 100-160 s. The same LNSW sample without OPA injected (red) shows the contribution of DOM and highlights the utility of rFIA for background fluorescence correction. The background fluorescence (red) can be significant and if not corrected for would lead to a positive bias of ~100 nM in this particular instance.

Fig. 2. The analytical manifold is diagramed above. The OPA reagent had a flow rate of 0.5 mL min^{-1}, the sample and the sulfite formaldehyde reagent had flow rates of 0.9 mL min^{-1}, and the waste tube had a flow rate of 2.1 mL min^{-1}.

Fig. 3. The effect of temperature on the slope of the calibration curve was determined by completing calibrations at 5 ℃ increments beginning with 45℃ and ending with 70 ℃. Plots a and b present the calibrations at various temperatures and the sensitivity versus temperature plots, respectively. The optimum temperature was determined to be 65 ºC.

Fig. 4. The effect of salinity on the slope of the calibration curve was determined by performing 7 standardizations using S=0.0, 3.0, 7.0, 13.0, 22.0, 30.0, and 39.0 LNSW diluted with polished DIW as the solvent. There is a slight increase in sensitivity with increased salinity, yet the low coefficient of determination indicates there is a low correlation between salinity and sensitivity.

Fig. 5. The standardization of the instrument was performed using a series of 6 solutions in triplicate: DIW, LNSW, 200 nM, 400 nM, 600 nM, and 800 nM ammonium. The ammonium standards were prepared in LNSW. The small double headed arrow indicates the fluorescent signal that is proportional to the dissolved organic matter. This background fluorescence is automatically subtracted from each sample, thereby improving the accuracy on nanomolar ammonium determinations (Masserini and Fanning, 2000).

Fig. 6. Calibration curve for the fluorescent ammonium rFIA calibration standards show in Fig. 4.

Fig. 7. The reagent stability with time was determined over a period of two months at 0, 16, 48, and 55 days from reagent preparation. The slope (nM/mV) increased to 48 days, then decreased at 55 days.

Fig. 8. Results of the surface surveys from the cruise described in the text on June 22, 2021. Plot a presents the regions of Tampa Bay that were sampled which included Hillsborough Bay (HB), Middle Tampa Bay (MTB), and Lower Tampa Bay (LTB). The location of Tampa Bay Land/Ocean Biogeochemical Observatory (LOBO) which provided temperature and salinity data is indicated by the green triangle. Plots b-d present ammonium concentrations (nM), fish kill (number of dead fish), and *K. brevis* cell concentration (cells L^{-1}), respectively. Plots were constructed using Ocean Data View (Schlitzer, 2021).

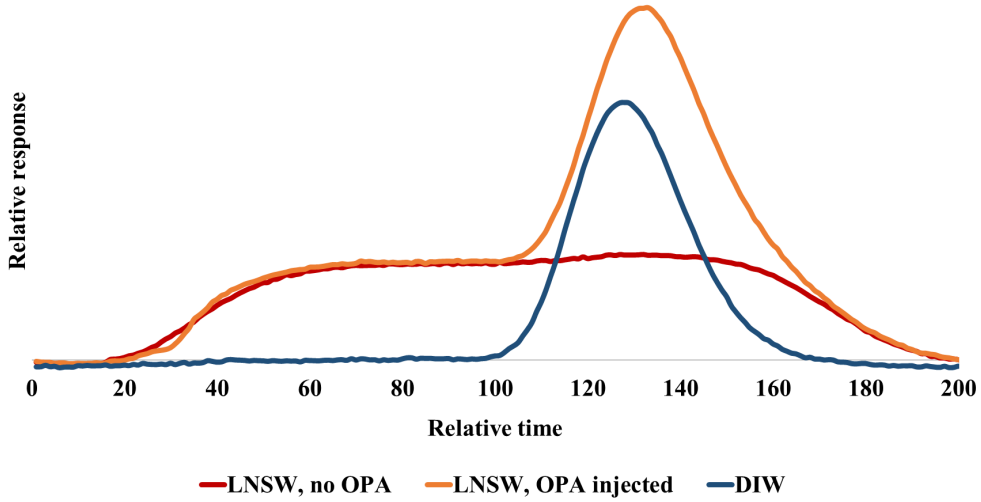
Relative response
0
20
40
60
80
100
120
140
160
180
200
Relative time
LNSW, no OPA
LNSW, OPA injected
DIW

Fig. 1

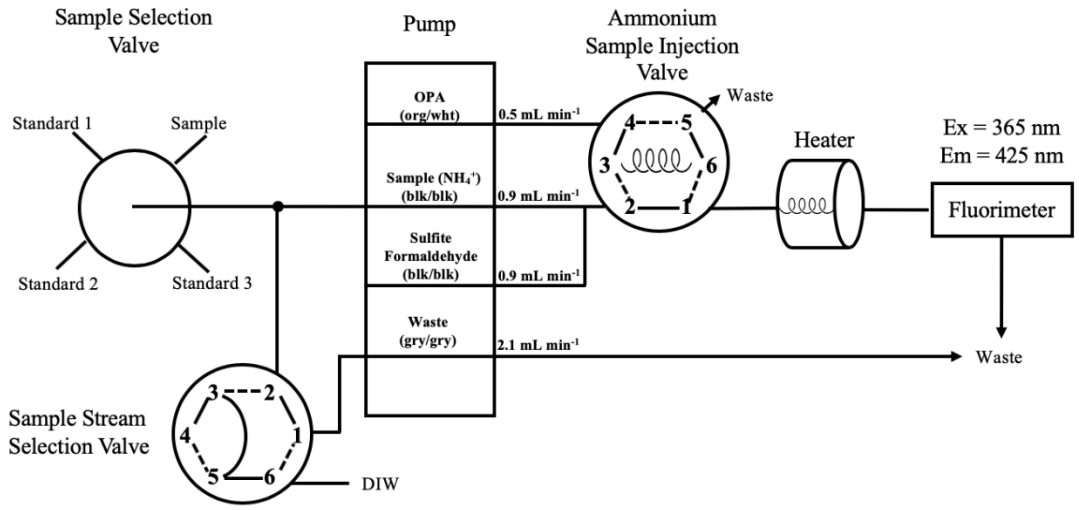
Sample Selection Valve
Pump
Ammonium Sample Injection Valve
Standard 1
Sample
Standard 2
Standard 3
OPA (org/wht)
0.5 mL min-1
Sample (NH4+) (blk/blk)
0.9 mL min-1
Sulfite Formaldehyde (blk/blk)
0.9 mL min-1
Waste (gry/gry)
2.1 mL min-1
Waste
Heater
Ex = 365 nm
Em = 425 nm
Fluorimeter
Waste
Sample Stream Selection Valve
DIW

Fig. 2

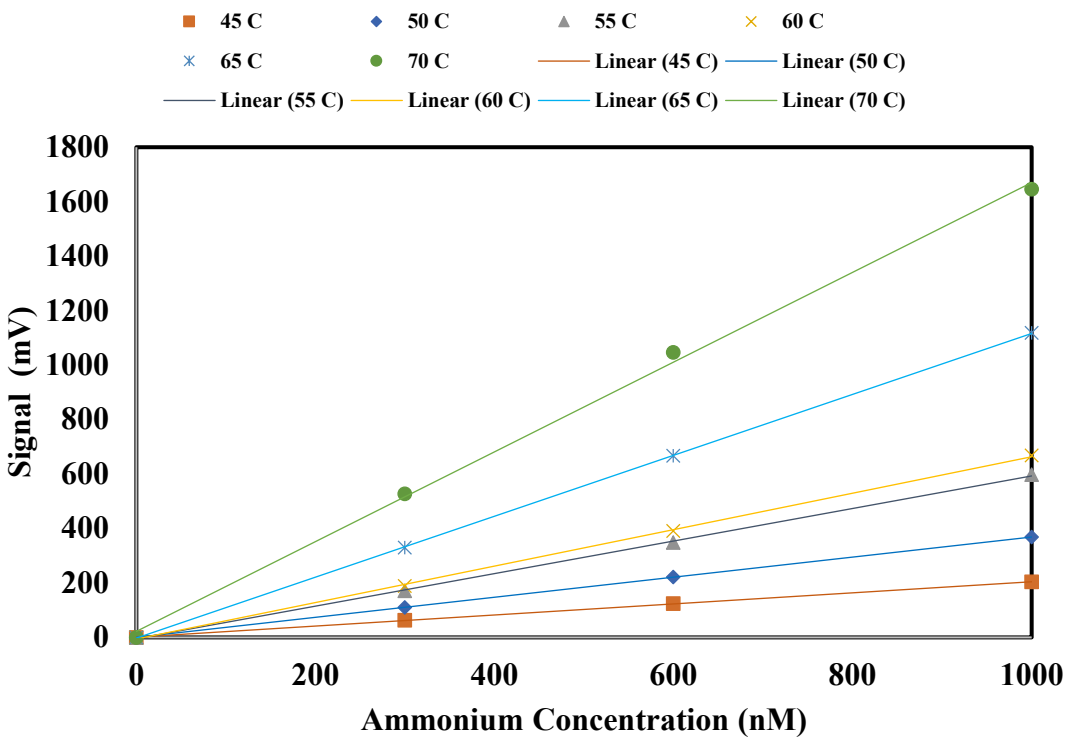
45 C
50 C
55 C
60 C
65 C
70 C
Linear (45 C)
Linear (50 C)
Linear (55 C)
Linear (60 C)
Linear (65 C)
Linear (70 C)
Signal (mV)
Ammonium Concentration (nM)

a.

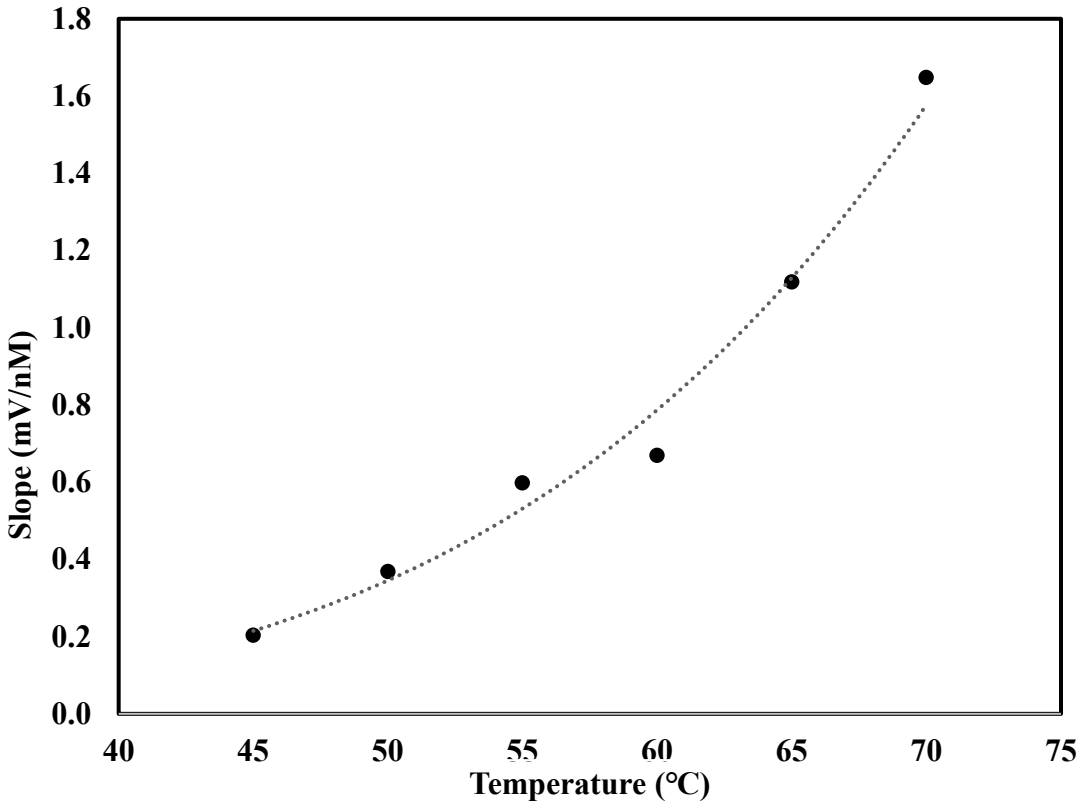
Slope (mV/nM)
Temperature (°C)

b.

Fig. 3

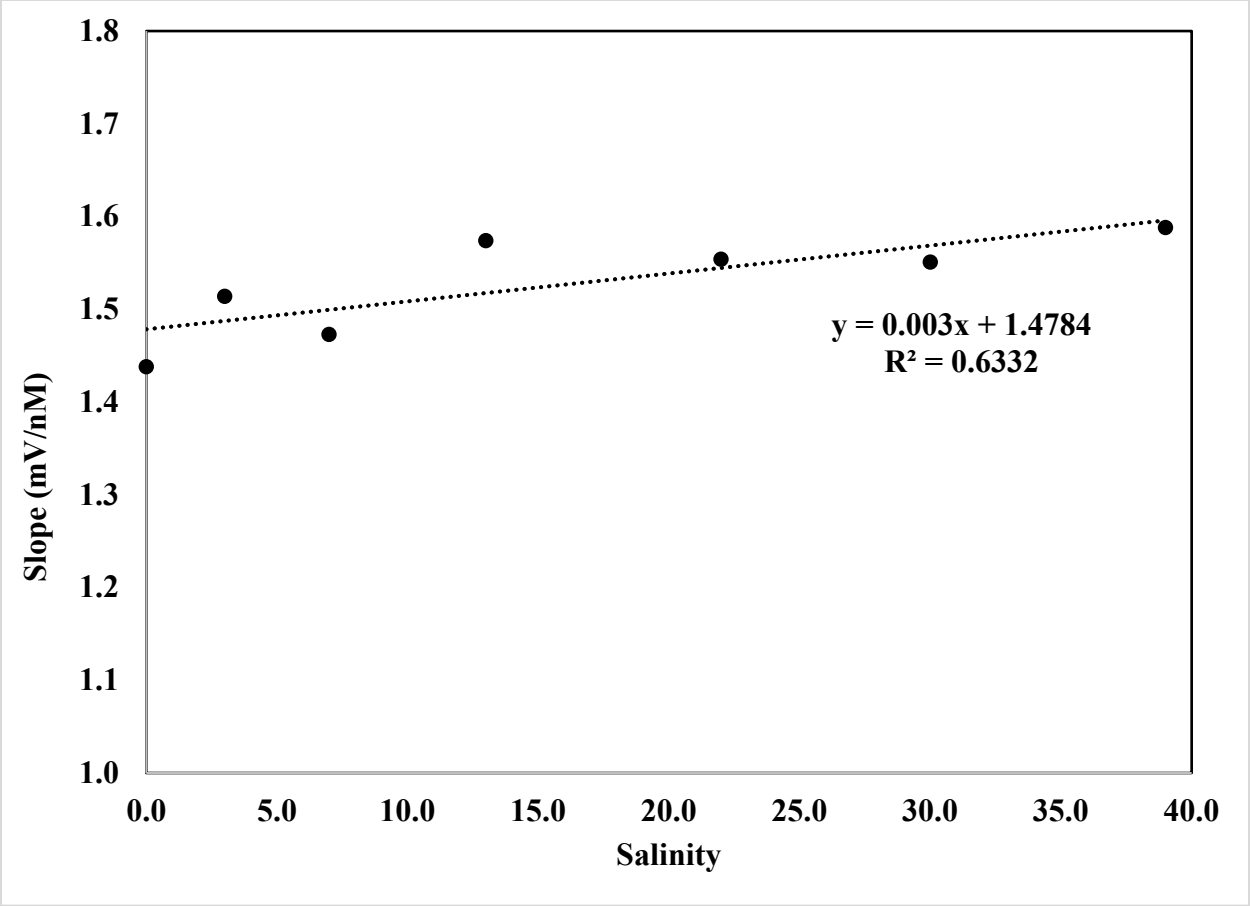
1.8
1.7
1.6
1.5
1.4
1.3
1.2
1.1
1.0
Slope (mV/nM)
y = 0.003x + 1.4784
R² = 0.6332
0.0
5.0
10.0
15.0
20.0
25.0
30.0
35.0
40.0
Salinity

Fig. 4

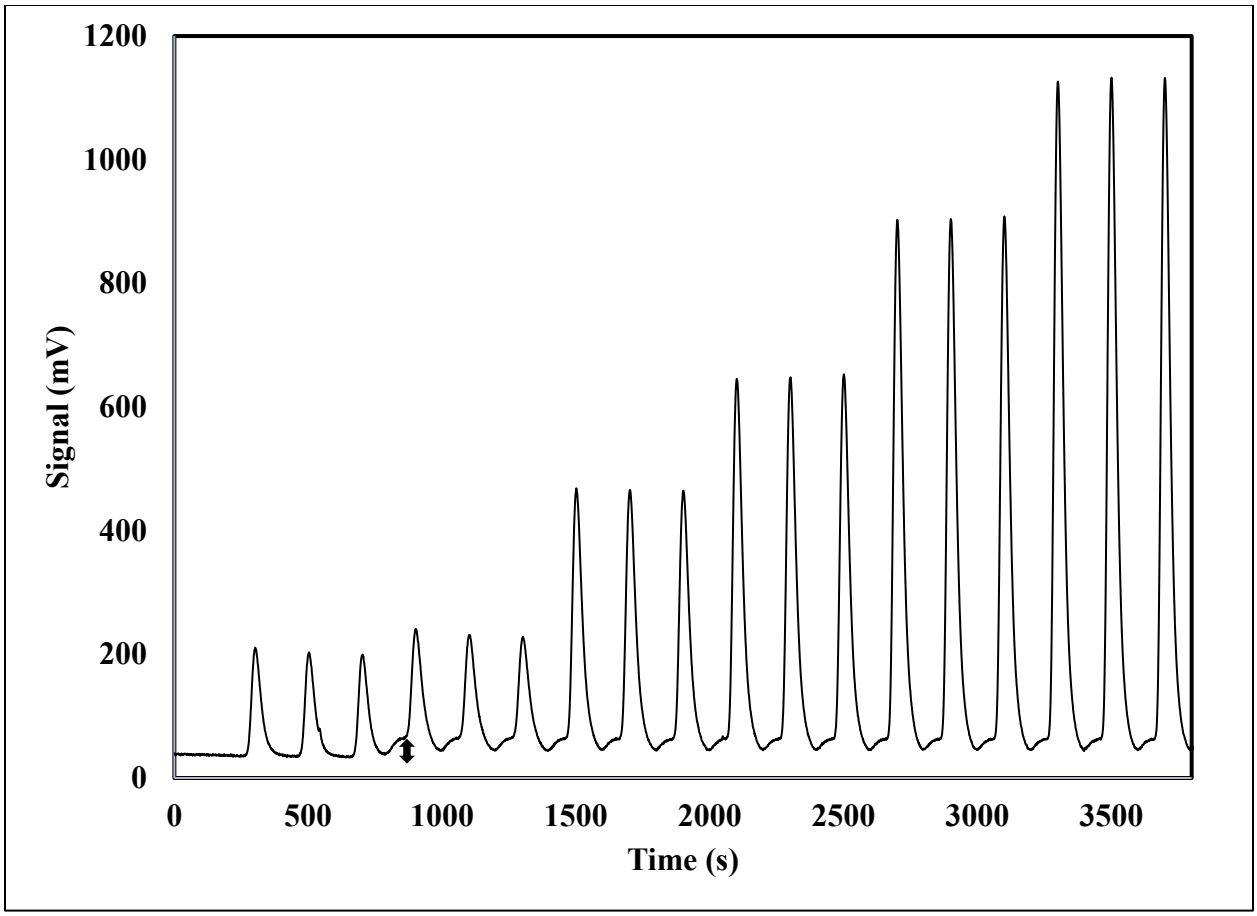
1200
1000
800
600
400
200
0
Signal (mV)
0
500
1000
1500
2000
2500
3000
3500
Time (s)

Fig. 5

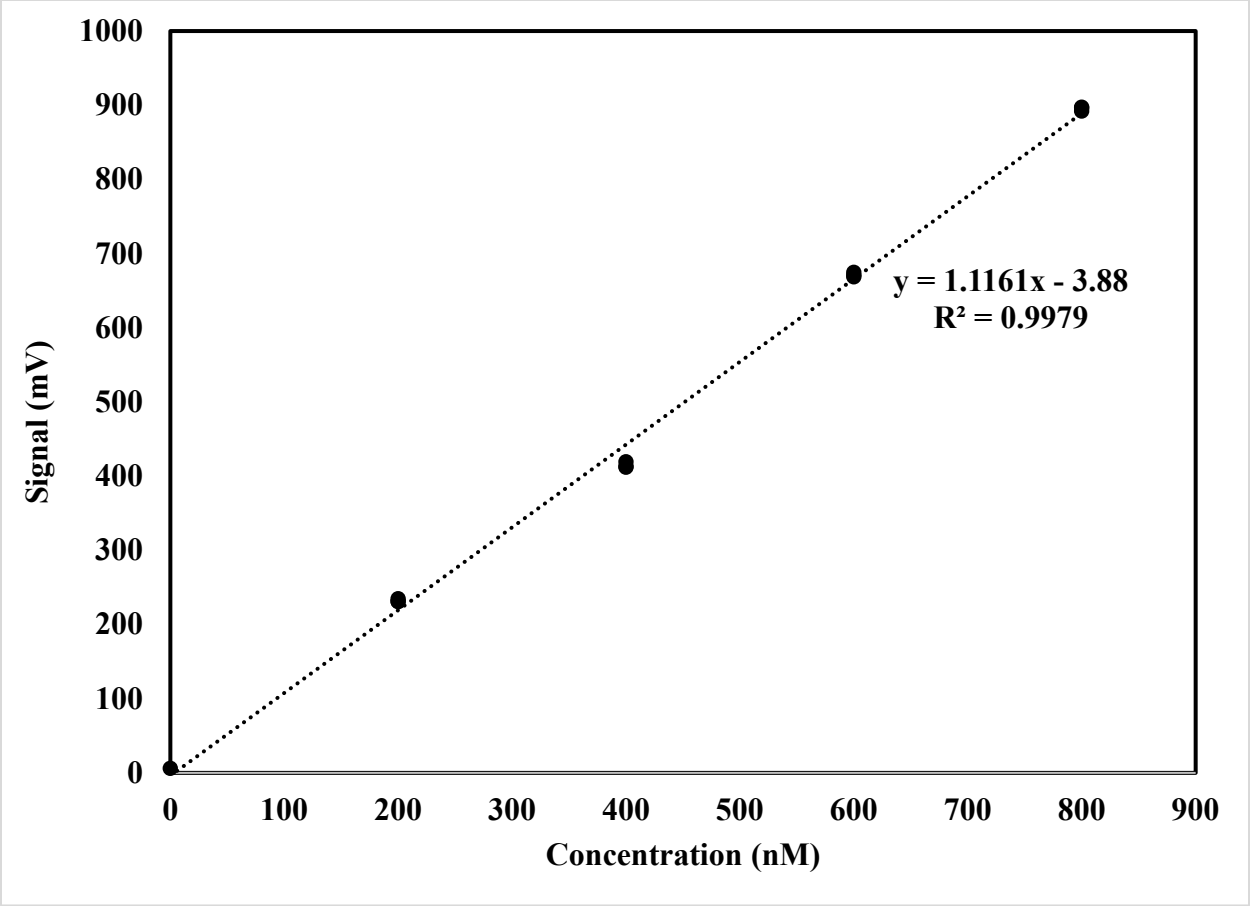
1000
900
800
700
600
500
400
300
200
100
0
Signal (mV)
y = 1.1161x - 3.88
R² = 0.9979
0
100
200
300
400
500
600
700
800
900
Concentration (nM)

Fig. 6

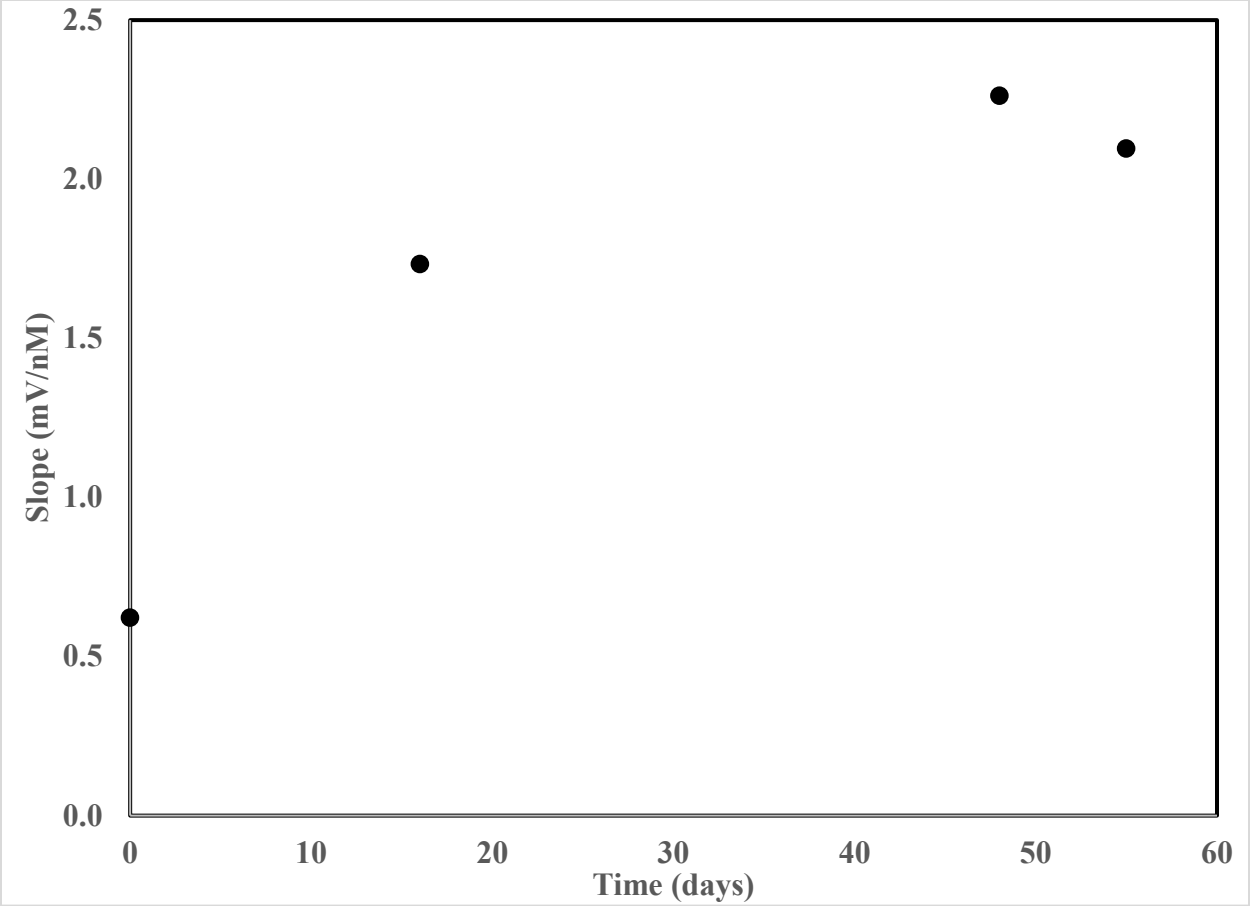

Fig. 7

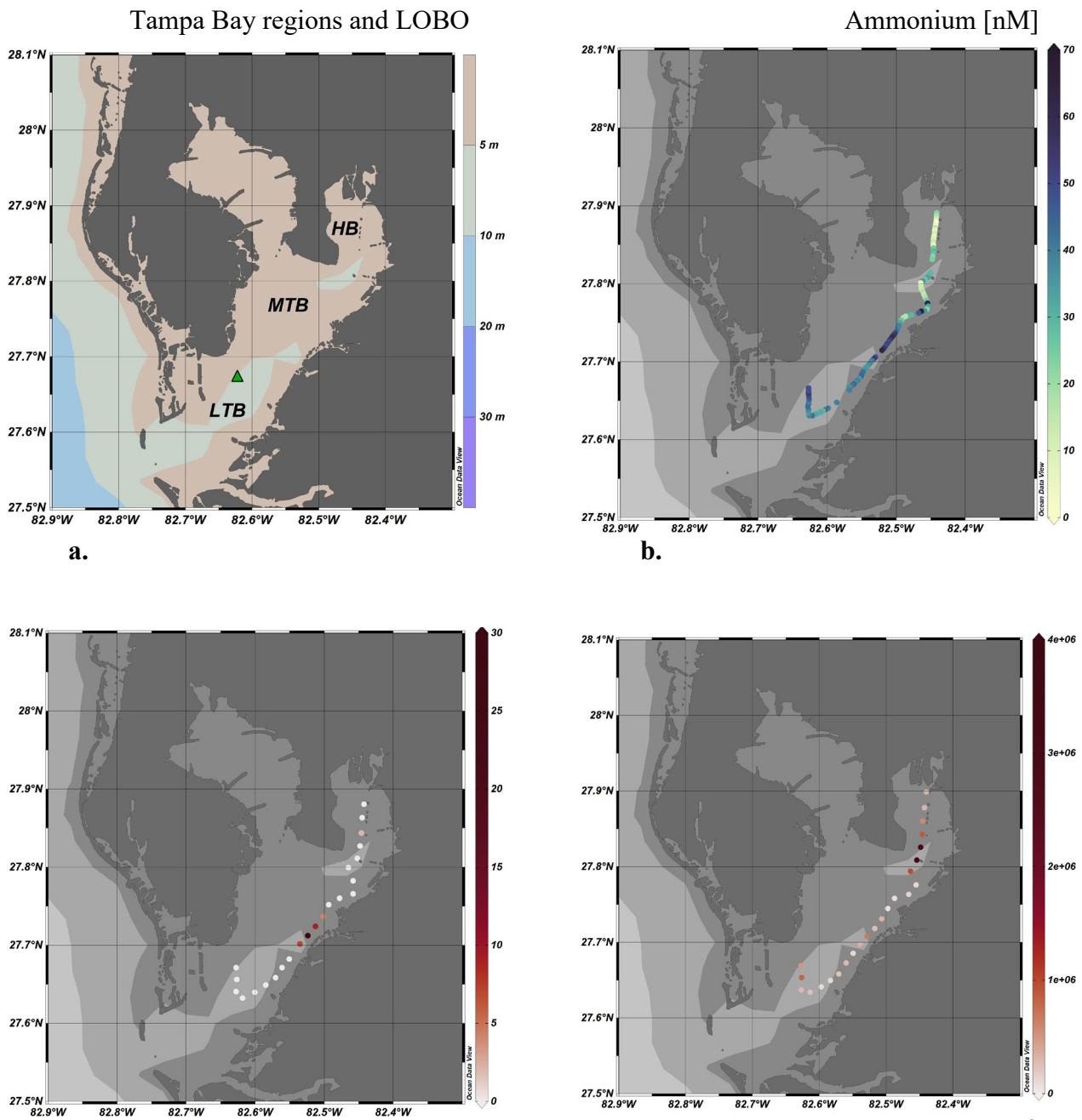
Tampa Bay regions and LOBO
HB
MTB
LTB
5 m
10 m
20 m
30 m
a.
Ammonium [nM]
b.
fish kill (counts)
c.
K. brevis cell concentration (cells L-1)
d.

Fig. 8